J Therm Anal Calorim (2012) 108:1017–1023
DOI 10.1007/s10973-011-1932-8

Investigation of Pd content in C–Pd films for hydrogen sensor applications

Ewa Kowalska · Elżbieta Czerwosz · Anna Kamińska · Mirosław Kozłowski

ICVMTT2011 Conference Special Chapter

Abstract Nanocomposite carbonaceous-palladium (Nc-C-Pd) films were synthesized by physical vapor deposition method (PVD). Scanning electron microscopy studies showed that they were composed of carbonaceous matrix containing Pd nanograins. Nc-C-Pd films were also characterized by thermogravimetric analysis, X-ray powder diffraction, and Fourier transform infrared (FTIR) spectral analysis. The content of Pd in films synthesized at different PVD conditions was determined based on TG measurements. Technological parameters of PVD process affected C/Pd ratio. FTIR spectra exhibited characteristic absorption bands for the precursors of carbonaceous-palladium samples (fullerene C_{60} and palladium acetate). The influence of hydrogen on electrical properties of the films was tested by measuring their resistance in the presence of hydrogen (1% H_2/N_2).

Keywords Carbonaceous-palladium films · Physical vapor deposition · Thermogravimetric analysis

Introduction

In the near future, hydrogen as an energy carrier could replace fossil fuels. In contrast to traditional fuels hydrogen burns to water and does not pollute the environment. Enormous financial resources in the European Union have been allocated to the specialized Programs associated with hydrogen technology (CUTE, HYPOGEN, HYCOM) [1–3].

Recently, hydrogen has been used in many industry branches connected with, e.g., hydrogenation process, chemical compounds production (NH_3, HCl, CH_3COOH), cryogenic cooling, metallurgy, and welding process and also in rocket engines [4]. Thus, continuous monitoring of the atmosphere composition near the hydrogen emission sources is necessary to preserve the industrial safety and protect human life. Sensors for monitoring and detection of dangerous gases could eliminate risk of explosion. These devices should be characterized by high sensitivity, fast response, and short regeneration time. Moreover, they should be cheap and simple in operation.

Currently available H_2 sensors have a response time of several seconds at 2% hydrogen content in atmosphere and have limitations and drawbacks depending on their constructions (e.g., semiconductor sensors show lack of selectivity, dependence of selectivity and sensitivity on temperature, and sensitivity change with the time) [5, 6]. Therefore, there is a need to develop a new kind of detectors that could measure the content of hydrogen and hydrogen compounds together.

An important factor for the detection sensitivity is well-developed surface area of active layers because it decides on the rate of a gas adsorption/desorption process. On the other hand, in case of hydrogen sensors, palladium is often applied as an component of the active layers because of its strongly reactivity toward hydrogen [7–9]. It is known that Pd creates palladium hydride PdH_x as a result of H_2 adsorption and next its absorption [10, 11]. The small activation barrier of the surface adsorption and the exothermal reaction of the inner absorption for palladium are together responsible for the palladium hydride formation. Some properties of PdH_x are different than pure Pd (e.g., conductance) [12] what allows to register the hydrogen presence in environment. It is worth noticing that Pd content as well as Pd nanograins size affects the sensitivity of sensor's active layers.

E. Kowalska (✉) · E. Czerwosz · A. Kamińska · M. Kozłowski
Tele and Radio Research Institute, Ratuszowa 11 Street, 03-450 Warsaw, Poland
e-mail: ewa.kowalska@itr.org.pl

Currently, new technologies and materials to produce multifunctional hydrogen sensors are searched for. In Tele and Radio Research Institute a new technology of preparation an active layer based on nanocomposite carbonaceous-palladium films (Nc-C-Pd films) is developed. Physical vapor deposition (PVD) process is applied to obtain the final films used as an active hydrogen sensing element.

In this study, we present the influence of changes of the distance between sources and substrates in PVD process on the composition of synthesized films especially on Pd content in carbonaceous materials.

Experimental

Samples synthesis method

Nc-C-Pd films were deposited on alumina substrates (Al_2O_3) during PVD process under the dynamic pressure of 10^{-5} mbar. Palladium(II) acetate ($PdC_4H_6O_4$, Sigma-Aldrich) was used as a precursor of palladium and fullerite C_{60} powder (99.99%, Sigma-Aldrich) was applied as a precursor of carbon. Both compounds were evaporated from two separated sources using electrical heaters.

PVD process proceeds in three stages: (1) formation of atomic/molecular vapor stream, (2) flow of atoms (molecules) from the vapor sources to substrates, and (3) condensation of vapor on substrates' surface and formation of films. In PVD deposition method parameters such as current flowing through both sources ($I_{C_{60}}$, I_{Pd}), duration (t) and the sources–substrates distance (d_{ss}) affects a structure quality and thickness of obtained films.

In our experiments only the distance d_{ss} was changed. The other technological parameters $I_{C_{60}}$, I_{Pd}, t) were the same in all processes (Table 1). Nanocomposite films containing carbonaceous grains and palladium nanoparticles with a diameter of 1–10 nm were formed as a result of PVD process. Transmission electron microscopy (TEM) results for such films were described in detail in our previous articles [13–15].

Table 1 Technological parameters of PVD samples synthesis method

No. samples	$I_{C_{60}}$/A	I_{Pd}/A	t/min	d_{ss}/mm
Sample 1	2.1	1.2	8	54
Sample 2	2.1	1.2	8	60
Sample 3	2.1	1.2	8	69

Characterization methods

The morphology and topography of Nc-C-P films were examined by scanning electron microscopy (SEM) with the JEOL JSM-7600F field emission scanning microscope, operating at 5 keV incident energy.

Thermogravimetric (TG) analysis was performed using SDT Q600 TA instruments in the temperature range 50–1,000 °C at the heating rate of 10 °C min^{-1}, both in argon atmosphere and in air. TG measurements were carried out at the gas flow rate of 100 cm^3 min^{-1} in alumina sample crucibles. Before each measurement the SDT system was equilibrated for 20 min at 50 °C.

Measurements in argon bring an information on a content of precursors (C_{60} and $PdC_4H_6O_4$) resting in Nc-C-Pd films after PVD process. Results obtained in the air atmosphere allow for calculating Pd content in these films assuming that all carbon in carbonaceous matrix was oxidized to CO_x ($x = 1$ or 2).

X-ray powder diffraction (XRD) technique using Siemens D500 diffractometer was applied to confirm the presence of Pd^0 in the samples after SDT measurements in air. XRD data were collected at room temperature in the $\theta/2\theta$ scanning mode with Cu K_α radiation and Si:Li semiconductor detector.

FTIR spectra were obtained with Thermo-Scientific Nicolet iS10 spectrometer using attenuated total reflectance (ATR) technique in the spectral range 650–4,000 cm^{-1} at the spectral resolution of 4 cm^{-1}. Spectra were 64 scanned and averaged to reduce the noise. Measurements were performed with Nc-C-Pd films deposited directly on alumina substrates.

Resistance of Nc-C-Pd samples was studied in hydrogen and the air atmosphere in an experimental set-up constructed in our laboratory. Measurements in hydrogen were performed at the room temperature and under atmospheric pressure using 1% hydrogen in nitrogen.

Results and discussion

Structure and morphology

In Figs. 1, 2, and 3 SEM images are presented for samples 1, 2, and 3, respectively. One can see that all samples despite of different distance d_{ss} in PVD method have similar structures. They consist of carbonaceous grains of size 100–150 nm distributed densely. The density of packing of C grains as well as their size seems to be the smallest in sample 3.

Thermal studies

TG/DTG curves of all samples obtained in argon atmosphere are shown in Fig. 4 whereas the same curves in the

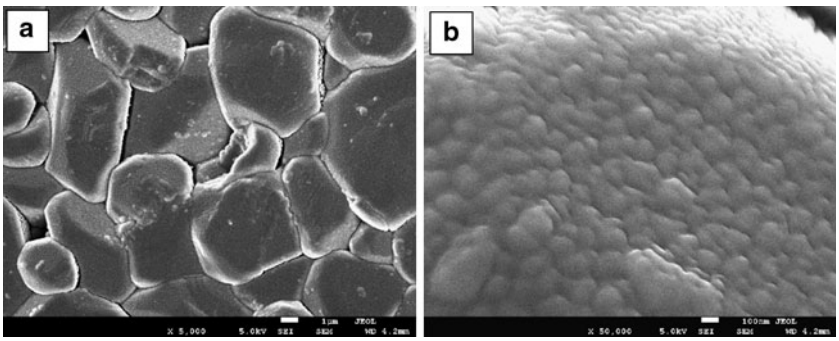

Fig. 1 SEM images of sample 1 ($d_{ss} = 54$ mm) with different magnifications: **a** ×5,000, **b** ×50,000

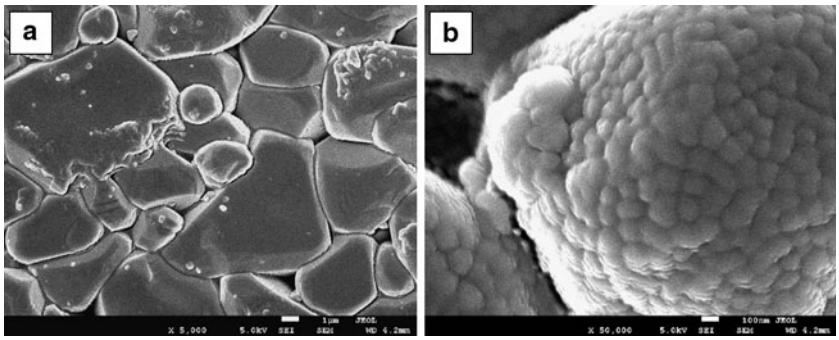

Fig. 2 SEM images of sample 2 ($d_{ss} = 60$ mm) with different magnifications: **a** ×5,000, **b** ×50,000

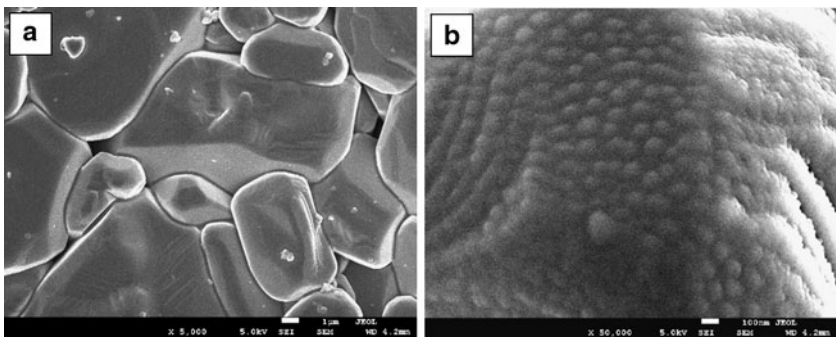

Fig. 3 SEM images of sample 3 ($d_{ss} = 69$ mm) with different magnifications: **a** ×5,000, **b** ×50,000

air are presented in Fig. 5. In Table 2, mass losses per temperature interval obtained by TG in argon atmosphere (columns 2, 3, and 4) and percent of samples' residue in argon (column 6) and in the air (column 7) are summarized. In addition, mass losses of films' precursors (C_{60} and $PdC_4H_6O_4$) are also given. In the last column (8), the mass ratio of C_{60}/Pd(II) acetate in samples obtained by PVD method is also presented.

In Fig. 4, we can see that mass loss of the samples in argon proceeds in three steps. The first step takes place at the temperature in range of 50–300 °C (Table 2, column 2). Accordingly to Gallagher publication [16] it is connected with decomposition of palladium acetate, which remained in Nc-C-Pd samples after PVD process. Observed mass loss in sample 1 is the smallest (11%wt) whereas in samples 2 and 3 it is similar (19–20%wt). Pd acetate content calculated from these mass losses indicates that sample 1 has 21% of palladium precursor while samples 2 and 3 contain from 35 to 38%wt of this compound (Table 2, column 5).

The second step occurs at the temperature in range of 300–500 °C and it can be related to mass loss of unidentified carbon fraction which may originate from C_{60} degradation during PVD synthesis. These mass losses are similar for all samples and they are 5.6–7.2%wt (Table 2 column 3).

The last mass loss is observed in a temperature region from 500 to 880 °C (Table 2, column 4) and it is attributed to C_{60} sublimation in an inert atmosphere [17]. Fullerene C_{60} (99.99% Sigma-Aldrich) used in our experiments had sublimation onset temperature at 727 °C whereas the temperature of the maximum rate of mass loss (peak DTG_{max}) was 792 °C. It could be observed that peak DTG_{max} ascribed to sublimation moves to higher temperatures for samples containing larger amount of fullerene.

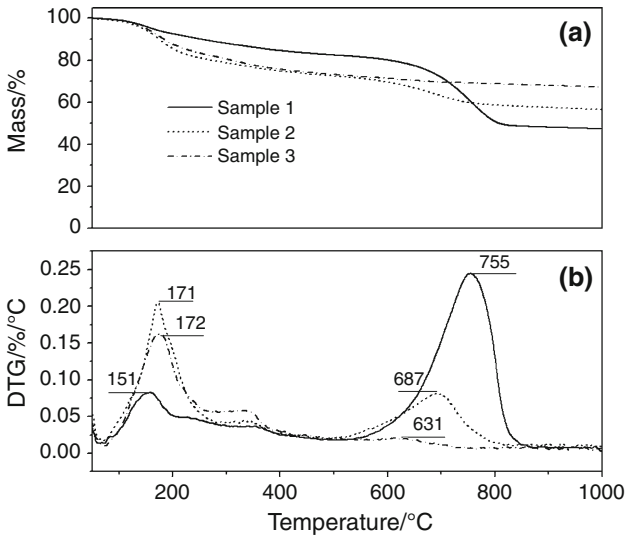

Fig. 4 **a** TG and **b** DTG curves of samples (1–3) in argon atmosphere with heating rate 10 °C min^{-1}

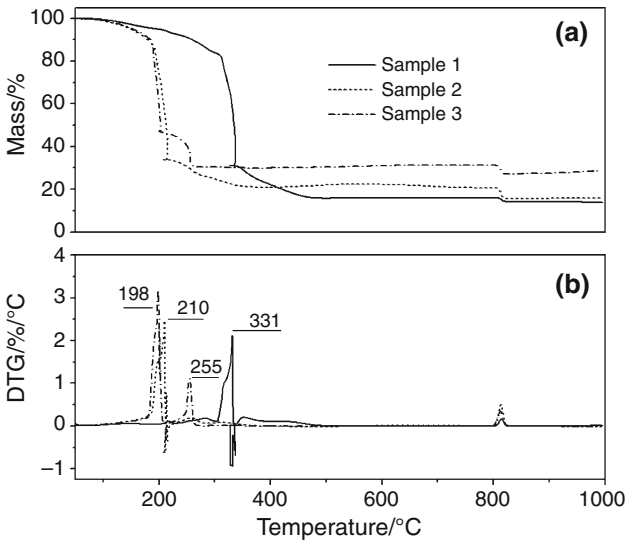

Fig. 5 **a** TG and **b** DTG curves of samples (1–3) in the air atmosphere with heating rate 10 °C min^{-1}

For example in sample 1 (34.1%wt of C_{60}—Table 2, column 4) peak DTG_{max} was found at 755 °C whereas in sample 3 (5.6%wt of C_{60}) it occurred at 631 °C. It is known that both the sublimation onset temperature as well as the temperature at maximum of DTG peak is different and they are dependent on fullerene quality (purity). In article [17], the C_{60} sublimation onset temperature in argon atmosphere with heating rate 10 °C min^{-1} was about 670 °C. Lower temperature of starting sublimation in comparison with our C_{60} sample is caused by the mixture of fullerenes (85% C_{60} + 15% C_{70}) used in TG analysis.

It results from TG measurements performed in argon (Fig. 5) that the distance sources–substrate in PVD method affects composition and also thermal stability of deposited films. The content of C_{60} in Nc-C-Pd samples decreases with the increase of d_{ss}. Sample 1 deposited at d_{ss} = 54 mm has the largest C_{60} content while in sample 3 deposited at d_{ss} = 69 mm the smallest amount of fullerene was found (Table 2, column 4). This effect is probably caused by higher molecular weight of fullerene (720 $gmol^{-1}$) comparing to the molecular weight of $PdC_4H_6O_4$ (224.5 $gmol^{-1}$). Thus, it is probable that fewer C_{60} molecules will reach the substrate placed in the larger distance from sources. Therefore, the mass ratio of C_{60} to Pd acetate decreases with the distance increase (Table 2, column 8).

The shape of TG/DTG plots in the air atmosphere (Fig. 5) is different and more complicated in comparison with profiles in argon. Peak DTG_{max}, attributed to decomposition of Pd acetate, occurs at higher temperatures especially in samples 1 and 2. In these measurements, there are difficulties in the separation of effects ascribed to C_{60} oxidation. TG/DTG plots registered in the air for fullerene sample used here (Sigma-Aldrich) were also carried out for comparison. Oxidation onset temperature was found at 484 °C while DTG_{max} connected with C_{60} combustion was observed at 537 °C. C. Sekar in article [18] showed that a temperature of C_{60} oxidation was 515 °C but in this case fullerene with a lower purity (92.8%) than here used C_{60} was studied.

In the presence of oxygen (Fig. 5), decomposition of $PdC_4H_6O_4$ (before 300 °C) may be connected with

Table 2 Mass losses per temperature interval obtained by TG in argon atmosphere (columns 2, 3, and 4), amount of samples' residue in argon (column 6) and in air (column 7), and calculated mass ratio of C_{60} to $PdC_4H_6O_4$ (column 8)

Sample No.	Mass loss in argon/%			Calculated content of $PdC_4H_6O_4$/%	Final residue/%		Ratio C_{60}: $PdC_4H_6O_4$
	50–300 °C	300–500 °C	500–880 °C		Argon	Air	
1	2	3	4	5	6	7	8
Sample 1	11	5.6	34.1	21	47.4	14	1.7
Sample 2	19.9	6.2	14.8	38.5	56.6	16	0.4
Sample 3	18.6	7.2	5.6	35.6	67.3	29	0.15
C_{60}	–	–	96.7	–	2.8	0.06	–
$PdC_4H_6O_4$	52.5	–	–	–	46	42	–

simultaneous oxidation of carbonaceous matrix. Only in sample 3, the first mass loss is ~52%wt with DTG_{max} at 198 °C and it is consistent with the release of organic parts ($C_4H_6O_4$ ~ 52.5%wt) in Pd acetate. In samples 1 and 2, containing higher amount of C_{60} than in sample 3, the first mass loss is greater than expected and is ~69%wt (DTG_{max} at ~331 °C) and ~66%wt (DTG_{max} at ~210 °C), respectively. Thus, we can conclude that decomposition of Pd acetate can occur simultaneously with C_{60} and carbon matrix combustion. The second mass loss about 12–15%wt with DTG peak at 351 °C (sample 1), 259 °C (sample 2), and 255 °C (sample 3) is probably connected with oxidation of C_{60} residue and unidentified carbon fraction. Above 400 °C, the interpretation of TG/DTG plots is difficult due to oxidization of Pd to PdO. Near 800 °C palladium oxide decomposed what was observed by Gallagher [16].

From TG data, we calculated that 11%wt of Pd in sample 3 was slowly oxidized for temperature higher than 400 °C. In the temperature above 800 °C, we observed little decrease in weight comparing with palladium mass at ~300 °C (after $PdC_4H_6O_4$ decomposition). This small mass loss (~10% of Pd mass) may occur due to a spontaneous reduction of PdO to Pd and simultaneous sublimation process of part of Pd [16]. The similar effect was also observed when only Pd acetate was heated in the air. In this case, mass of Pd at temperatures higher than 800 °C is smaller (about 7%wt) than mass at temperature of 300 °C.

The final samples' residue in the air at temperature of 1,000 °C (after TG measurements) contained pure palladium grains with *fcc* structure what was determined by powder XRD analysis (Fig. 6). The highest mass of the residue was found in sample 3 (29%wt –Table 2, column 7) whereas sample 1 had the smallest amount of the residue (14%wt). Thus, palladium content in sample 3 deposited at $d_{ss} = 69$ mm was the highest. It is probably caused by the lowest C_{60} content in this sample, what was confirmed by TG analysis in argon.

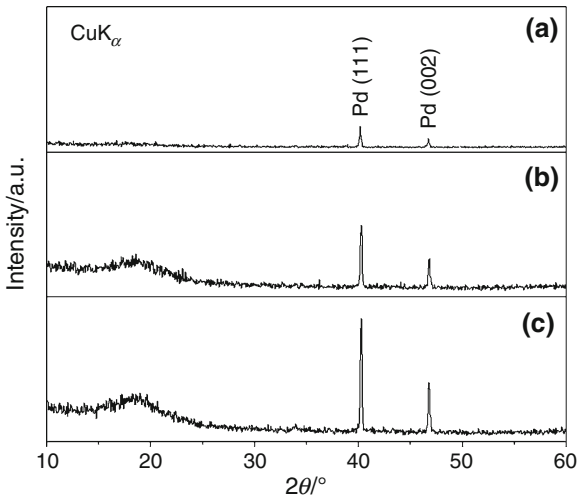

Fig. 6 X-ray diffraction pattern of the residues from TG analysis performed in the air atmosphere: **a** sample 1, **b** sample 2, and **c** sample 3

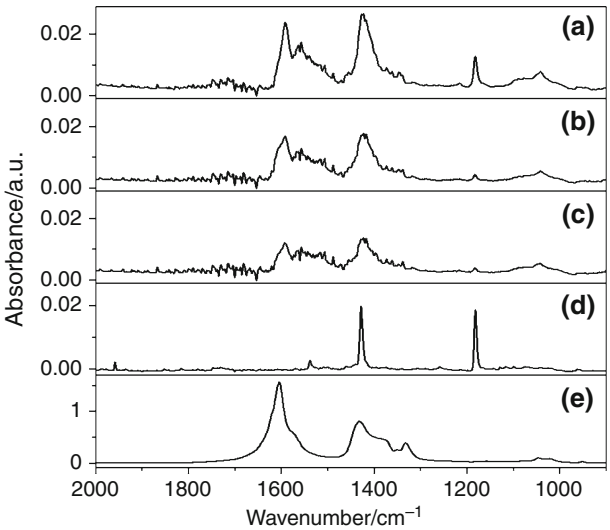

Fig. 7 FTIR/ATR spectra of samples and films' precursors: **a** sample 1, **b** sample 2, **c** sample 3, **d** fullerene C_{60}, and **e** $PdC_4H_6O_4$

FTIR analysis

FTIR spectra of all samples (1–3) and of films' precursors (C_{60} and $PdC_4H_6O_4$) are presented in Fig. 7. The spectrum of C_{60} (Fig. 7d) shows sharp, very narrow bands at wavenumbers of 1,183 and 1,428 cm^{-1} assigned to the T_{1u} vibrational mode [19]. The other C_{60} characteristic bands placed at 525 and 577 cm^{-1} are out of measuring range using ATR method. Spectrum corresponding to Pd acetate (Fig. 7e) exhibits three dominating absorption bands: (1) broad band placed between wavenumbers of 1,640 and 1,570 cm^{-1} associated with the asymmetric stretching vibrations of C=O bond in the ionized carboxylate groups (CH_3COO^-); (2) band placed at 1,430 cm^{-1} attributed to the symmetric stretching vibrations of the same bond (C=O), and (3) band found at 1,335 cm^{-1} connected to the CH_3 bending vibration [20].

The bands connected to C_{60} (1,183 cm^{-1}) and Pd acetate (1,590 and 1,420 cm^{-1}) molecules vibrations were found in spectra of studied samples (Fig. 7a–c) obtained by PVD process using various distances d_{ss}. Only narrow band at wavenumber 1,428 cm^{-1} characteristic for fullerene vibration is not visible due to overlaps with band associated with the symmetric stretching vibrations of C=O bond in the CH_3COO^- anion (Pd acetate).

FTIR analysis confirms that films' precursors are present in samples deposited on substrates by PVD method what is consistent with TG measurements.

On the basis of FTIR spectral analysis, we can not estimate the concentration of C_{60} and Pd acetate in the samples because the intensity of bands depends not only on the content of the specific component of the sample but also on the sample's thickness and absorption coefficients. It is possible that with the distance d_{ss} increase the thickness of samples decreases because less and less molecules reach substrates. Therefore, we can only calculate the ratio of intensity bands attributed to fullerene (1,183 cm^{-1}) and palladium acetate (1,420 cm^{-1}) (Table 3) and check C_{60} concentration in relation to Pd acetate content. Calculated intensity ratio ($In_{C_{60}}/In_{PdC4H6O4}$) decreases with increasing d_{ss} because of the decrease of C_{60} content in the samples. This observation confirms results obtained from TG analysis (Table 2, column 8).

Electrical properties

The sample 3 due to the highest Pd concentration (29%wt) was chosen to study the changes of its resistance under the influence of hydrogen (Fig. 8). We expected that the high Pd content allows for easier observation of the film response to the hydrogen presence.

Relative resistance ΔR was calculated by the following formula:

$$\Delta R\ [\%] = \frac{R(t) - R(t_0)}{R(t_0)} \cdot 100\%$$

where $R(t)$ is the sample resistance exposed to gas for time t, $R(t_0)$ is the sample initial resistance in hydrogen absence.

From Fig. 8, results that the resistance of sample 3 increases under hydrogen atmosphere and next decreases as the result of H_2 desorption while the air is introduced into the measuring chamber. The changes of ΔR at hydrogen presence were approximately 6%. The observed increase of the film resistance could be caused by adsorption of H_2 and creation of palladium hydride PdH_x. As it was shown in article [12], PdH_x exhibited higher resistance in comparison with metallic palladium. It is worth to note that the sample resistance after each adsorption–desorption cycle returns to its initial value. Thus, we can conclude about total H_2 desorption from the sample. These results show that studied films can find wide applications as an active layer in hydrogen sensors.

Table 3 The ratio of intensity bands ascribed to C_{60} (1,183 cm^{-1}) and $PdC_4H_6O_4$ (1,420 cm^{-1})

Sample No.	$In_{C_{60}}/In_{PdC4H6O4}$
Sample 1	0.47
Sample 2	0.14
Sample 3	0.13

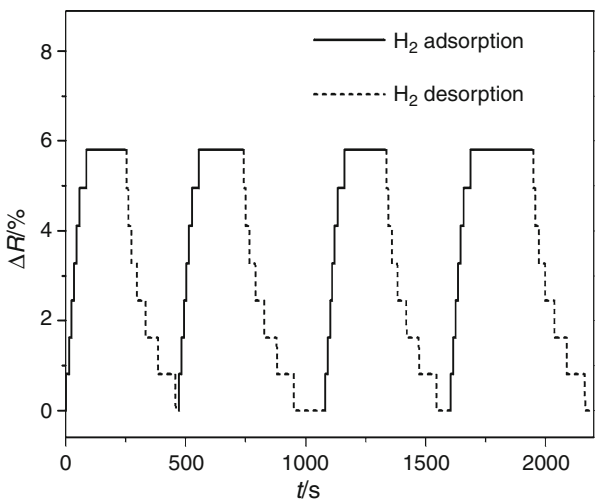

Fig. 8 Changes of sample 3 resistance under 1% H_2 in nitrogen

Conclusions

We develop the technology for obtaining thin films (based on carbonaceous materials and Pd nanograins) that can be applied as active layers in hydrogen sensors. Therefore, diagnostic methods to correct technological parameters of PVD process are searched for. TG analysis performed in argon is a suitable method to determine the concentration of films' precursors (C_{60} and $PdC_4H_6O_4$) in studied samples whereas TG measurements in the air allow for determining Pd content in them.

We noticed that Pd concentration in Nc-C-Pd samples increases with increasing the distance between sources and substrates in PVD chamber. This result is caused not only by decreasing C_{60} content in these samples but also by decreasing mass ratio of C_{60} to Pd acetate with the increase of d_{ss}. We suggest that differences in molecular weight of both precursors are responsible for observed changes in the samples' composition. The sample with the highest Pd content was tested for use it as an active layer in hydrogen sensor. As a result of reaction with hydrogen electrical properties of this sample was changed. Thus, sample containing the highest Pd content can be applied as active layer in hydrogen sensors.

Authors thank Dr. Ryszard Diduszko (Tele and Radio Research Institute) for X-ray diffraction measurements.

Acknowledgements This project is co-financed by the European Regional Development Fund within the Innovative Economy Operational Programme 2007–2013 (title of the project "Development of technology for a new generation of the hydrogen and hydrogen compounds sensor for applications in above normative conditions" No UDA-POIG.01.03.01-14-071/08-06).

References

1. http://www.global-hydrogen-bus-platform.com/.
2. ftp://ftp.cordis.europa.eu/pub/fp7/energy/docs/hydrogen_synopses_en.pdf.
3. http://setris.jrc.ec.europa.eu/docs/files/EUR21575EN.pdf.
4. Sayago I, Terrado E, Lafuente E, et al. Hydrogen sensor based on carbon nanotubes thin films. Synth Met. 2005;148:15–9.
5. Brzózka Z, Wróblewski W. Sensory chemiczne. Warszawa: Oficyna Wydawnicza Politechniki Warszawskiej; 1998.
6. Janata J. Principles of chemical sensors. New York: Plenum Press Inc.; 1989.
7. Rather S, Zacharja E, Hwang SW, et al. Hyperstoichiometric hydrogen storage in monodispersed palladium nanoparticles. Chem Phys Lett. 2007;438:78–84.
8. Luongo K, Sine A, Bhansali S. Development of a highly sensitive porous Si-based hydrogen sensor using Pd nano-structures. Sens Actuator B-Chem. 2005;111–112:125–9.
9. Pavlovsky I, Soundarrajan P, Yaniv Z. Palladium nanoparticle hydrogen sensor. Sens Transducers J. 2006;73:793–8.
10. Sachs C, Pundt A, Kirchheim R, et al. Solubility of hydrogen in single-sized palladium clusters. Phys Rev B. 2001;64:075408.
11. Kishore S, Nelson JA, Adair JH, Eklund PC. Hydrogen storage in spherical and platelet palladium nanoparticles. J All Comp. 2005;389:234–8.
12. Ibanez FJ, Zamborini FP. Ozone- and thermally activated films of palladium monolayer-protected clusters for chemiresistive hydrogen sensing. Langmuir. 2006;22:9789–96.
13. Czerwosz E, Dłużewski P, Kęczkowska J, et al. Palladium nanocrystals and their properties. Mater Sci. 2008;1:19–125.
14. Czerwosz E, Diduszko R, Dłużewski P, et al. Properties of Pd nanocrystals prepared by PVD method. Vacuum. 2008;82:372–6.
15. Kowalska E, Czerwosz E, Kozłowski M, et al. Structural, thermal, and electrical properties of carbonaceous films containing palladium nanocrystals. J Therm Anal Calorim. 2010;101:737–42.
16. Gallagher PK, Gross ME. The thermal decomposition of palladium acetate. J Therm Anal. 1986;31:1231–41.
17. Cuesta A, Jamond M, Martinez-Alonso A, Tascon JMD. Thermal behavior of fullerenes in different gas atmosphere. Carbon. 1996;34:1239–48.
18. Sekar C, Subramanian C. Purification and characterization of buckminsterfullerene, nanotubes and their by products. Vacuum. 1996;47:1289–92.
19. Jing D, Pan Z. Molecular vibrational modes of C_{60} and C_{70} via finite element method. Eur J Mech A-Solid. 2009;28:948–54.
20. Fang Q, He G, Cai WP, et al. Palladium nanoparticles on silicon by photo-reduction using 172 nm excimer UV lamps. Appl Surf Sci. 2004;226:7–11.